THE JOURNAL OF PHYSICAL CHEMISTRY B

Article

pubs.acs.org/JPCB

Critical V_2O_5/TeO_2 Ratio Inducing Abrupt Property Changes in Vanadium Tellurite Glasses

Jonas Kjeldsen,[†] Ana C. M. Rodrigues,[‡] Susanne Mossin,[§] and Yuanzheng Yue*[,†,∥]

[†]Section of Chemistry, Aalborg University, DK-9000 Aalborg, Denmark

[‡]Department of Materials Engineering, Federal University of São Carlos, C.P. 676, 13565-905 São Carlos, SP, Brazil

[§]Department of Chemistry, Technical University of Denmark, 2800 Kongens Lyngby, Denmark

[∥]State Key Laboratory of Silicate Materials for Architecture, Wuhan University of Technology, Wuhan 430070, China

ABSTRACT: Transition metal containing glasses have unique electrical properties and are therefore often used for electrochemical applications, such as in batteries. Among oxide glasses, vanadium tellurite glasses exhibit the highest electronic conductivity and thus the high potential for applications. In this work, we investigate how the dynamic and physical properties vary with composition in the vanadium tellurite system. The results show that there exists a critical V_2O_5 concentration of 45 mol %, above which the local structure is subjected to a drastic change with increasing V_2O_5, leading to abrupt changes in both hardness and liquid fragility. Electronic conductivity does not follow the expected correlation to the valence state of the vanadium as predicted by the Mott−Austin equation but shows a linear correlation to the mean distance between vanadium ions. These findings could contribute to designing optimum vanadium tellurite compositions for electrochemical devices. The work gives insight into the mechanism of electron conduction in the vanadium tellurite systems.

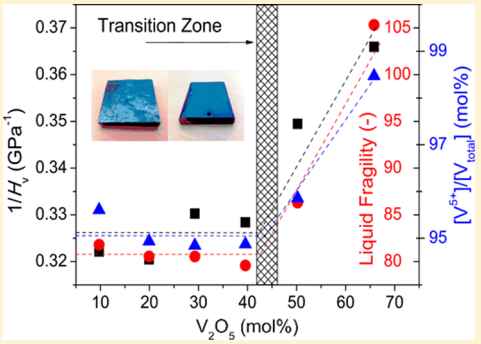

1. INTRODUCTION

Transition metal containing oxide glasses exhibit a unique set of optical and electrical properties.[1−7] Owing to their high electronic conductivity, they have often been applied in electrochemical devices.[8−15] In particular, vanadium tellurite glasses show higher electronic conductivity than other vanadium containing oxide glasses such as phosphates, borates, and silicates[16−21] and therefore have attracted much attention of scientists.[3−9,11−13] The compositional dependence of hardness in the TeO_2−V_2O_5 glass system has been studied to some extent.[22,23] The structure of this glass system has been determined using nuclear magnetic resonance spectroscopy, neutron and X-ray diffraction, and Raman spectroscopy.[24−26] In the vanadium tellurite system, the effect of the composition on glass transition temperature (T_g) has been explored,[3,27,28] and the liquid fragility index (m), i.e., the speed of the viscosity change at T_g upon cooling or heating, has been determined.[3,4] More recently, the electronic conductivity of $2TeO_2$−V_2O_5 glass ceramics was studied as a function of the degree of crystallinity.[29] To the best of our knowledge, a systematic study has not been reported concerning the compositional dependence of both static and dynamic properties of vanadium tellurite glasses. In order to better understand the composition−structure−property relationship of this glass system and thereby tailor its electrochemical performance, it is necessary to perform a thorough study of the dynamic, electrical, and physical properties. Another interesting aspect of this study is to verify whether the vanadium tellurite liquids are indeed so fragile as reported in previous studies.[3,4,29] If this is the case, we should explore the structural origin of the high fragility of these glass liquids.

In this study, we determine the valence state ratio of vanadium (c), m, T_g, Vickers hardness (H_v), density (ρ), electronic conductivity (σ), and glass stability via the Hrüby parameter (K_H) of vanadium tellurite glasses. We focus on the compositional dependences of these properties and explain their structural origin. The knowledge gained from this work could be used for designing vanadium tellurite glass compositions for electrochemical devices.

2. EXPERIMENTAL SECTION

Glass samples were prepared via the melt quenching technique, using reagent grades of ≥99.6% V_2O_5 and ≥99.5% TeO_2. A series of V_2O_5−TeO_2 glasses with various V_2O_5 contents were synthesized by mixing and milling the batches of both oxide materials for 0.25 h, melting them at 800 °C for 0.5 h, quenching the melt on a brass plate, and finally annealing the formed glasses for 2 h at their respective T_g. The amorphous state of all glasses was verified by X-ray diffraction (Rigaku, Ultima IV) using Cu Kα radiation, and their final chemical compositions were determined by energy dispersive X-ray spectroscopy (Phenom). The analyzed chemical compositions are given in Table 1. Compositions are described by the molar percentage of vanadia, namely, $X = [V_2O_5]/([V_2O_5] +$

Received: September 3, 2014
Revised: October 22, 2014
Published: November 27, 2014

Table 1. Chemical Composition of the Six Vanadium Tellurite Glasses with Various V_2O_5 Contents[a]

sample name	V_2O_5 [mol %]
VT_10	9.7
VT_20	19.9
VT_30	29.2
VT_40	39.6
VT_50	50.2
VT_65	65.8

[a]The compositions were analyzed by energy dispersive X-ray spectroscopy (±0.3 mol %).

$[TeO_2]$). Room-temperature density was determined by gas pycnometry (Quantachrome, Ultrapyc 1200e) using helium as pressure gas.

Coplanar samples of each composition were polished and sputtered with gold before electronic conductivity was measured by impedance spectroscopy (Solartron, SI1260). The electrical measurements were performed in air with a two-point sample holder from 303 to 523 K and with an applied voltage of 100 mV in the frequency range from 10^6 to 1 Hz. Impedance data were plotted in an impedance complex plane (Nyquist diagram) and fitted by an equivalent circuit consisting of one resistor in parallel with one capacitor. The dc resistances (R_s) were thus determined by the intercept of the semicircle to the real axis at low frequency. σ was calculated as $\sigma = (1/R_s)(l/S)$ (l and S are the thickness and the surface area of the sample in contact with the electrode, respectively). H_v was measured via a Knoop pyramid indenter (Duramin, Struers). A total of 30 indents were made on each sample using an indentation time of 10 s and an indentation load of 0.25 N. The measurements were performed in air at room temperature.

The liquid fragility indices were determined by a linear fitting of the viscosity data around T_g. The viscosities in the range of $\eta = 10^{11}-10^{13}$ Pa s were measured using a ball penetration viscometer (Bähr, Vis 405). For each data point, a minimum of five penetrations were made at a specific temperature. The pressing ball was made of silica. Press depth was 300 μm, and the press load was between 2 to 9 N.

Calorimetric measurements were performed on a differential scanning calorimeter (DSC) (Jupiter 449C, Netzsch) in order to determine the calorimetric glass transition temperature (T_g), the crystallization onset temperature (T_c), the melting onset temperature (T_m), and the isobaric heat capacity jump during the glass transition (ΔC_p). Each sample was initially subjected to an upscan to 700 °C at 10 K/min in order to determine T_c and T_m. Subsequently each composition is subjected to a downscan and an upscan at 10 K/min to approximately 100 K above T_g. The first upscan curves reflect the thermal history of an unknown cooling rate, whereas the second upscan curves reflects the standard thermal history of a cooling of 10 K/min during the first downscan.[30] A flow of 40 mL/min argon was used as protective gas, and gold crucibles were used for both sample and reference. Both T_g and ΔC_p were determined from the second upscan. In order to calculate the isobaric heat capacity (C_p) of the vanadium tellurite glasses, a 63 mg sapphire standard was utilized.

The concentration of V^{4+} was determined by electron paramagnetic resonance (EPR) spectroscopy. For each sample approximately 20 mg of powder was measured at room temperature in a Bruker EMX X-band EPR spectrometer with an ER 4102ST cavity and a Gunn-diode microwave bridge. The spectra were obtained from 2850 to 3500 G at microwave frequency 9.58 GHz, microwave power 6.31 mW, modulation frequency 100 kHz, and modulation width 8 G and were accumulated over 10 sweeps. Identical settings were used for five standards containing known concentrations of $VO(SO_4)\cdot 3H_2O$ (Sigma-Aldrich) in K_2SO_4 (Sigma-Aldrich).

3. RESULTS

Figure 1 shows the first DSC upscans of the vanadium tellurite glasses. T_c is defined as the crystallization onset temperature,

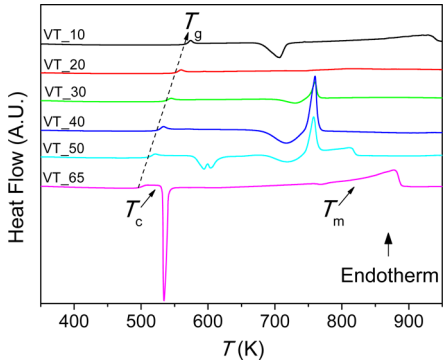

Figure 1. Differential scanning calorimetry upscans at 10 K/min of the vanadium tellurite glasses. Curves are translated on the ordinate for comparison. An example of the determination of the characteristic calorimetric temperatures (T_g, T_c, and T_m) is shown in the inset of Figure 2

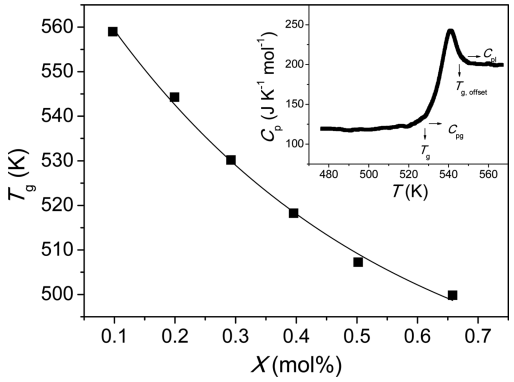

Figure 2. Glass transition temperature (T_g) as a function of X ($=[V_2O_5]/([V_2O_5] + [TeO_2])$) of the vanadium tellurite glasses. The solid line is a guide for the eye showing the compositional scaling of T_g. Inset: Determination of the C_p jump during the glass transition, i.e., $\Delta C_p = C_{pl} - C_{pg}$,[30] taking the 30 mol % V_2O_5 glass as an example. The error range of the T_g values is ±2−3 K.[31]

whereas T_m is determined as the onset temperature of the melting peak. Figure 2 demonstrates the nonlinear dependence of T_g on the V_2O_5 content of the vanadium tellurite glasses. The inset illustrates how to determine the C_p jump during the glass transition, i.e., $\Delta C_p = C_{pl} - C_{pg}$, where C_{pl} and C_{pg} respectively are the isobaric heat capacities of the liquid and the glass at T_g. ΔC_p is a measure of the thermodynamic liquid fragility.[31] The C_p curves for all glasses are shown in Figure 3. On the basis of the characteristic temperatures obtained in Figure 1, the Hrüby parameter (K_H) is determined. K_H is a measure of the glass stability against crystallization as determined by the following equation, which has a positive relation with the glass forming ability of a given system:[32−34]

dx.doi.org/10.1021/jp508910m | J. Phys. Chem. B 2014, 118, 14942−14948

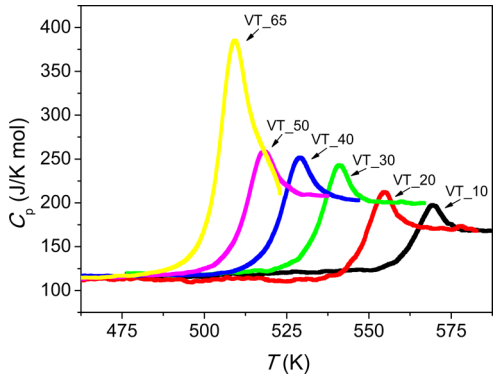

Figure 3. Isobaric heat capacity (C_p) as a function of temperature (T), which was determined during the second DSC upscans at 10 K/min following the prior downscan at 10 K/min for the six vanadium tellurite glasses under study (see Table 1).

$$K_H = \frac{T_c - T_g}{T_m - T_c} \quad (1)$$

K_H and ΔC_p values are listed in Table 2. The dependence of K_H on X obeys a gauss distribution with a maximum very close to the congruent composition of V_2O_5–$2TeO_2$.[35]

Table 2. Glass Transition Temperature (T_g), Crystallization Onset Temperature (T_c), Melting Onset Temperature (T_m), Glass Stability Parameter (K_H), and Heat Capacity Jump at T_g (ΔC_p) Obtained from Differential Scanning Calorimetry

sample name	T_g [K]	T_c [K]	T_m [K]	K_H [−]	ΔC_p [J mol^{-1} K^{-1}]
VT_10	559	679	858	0.7	41.2
VT_20	544	688	740	2.8	58.3
VT_30	530	704	750	3.7	82.6
VT_40	518	682	746	2.6	97.1
VT_50	507	578	743	0.4	96.4
VT_65	500	531	746	0.1	191.6

In Figure 4 $c = [V^{4+}]/[V_{total}]$ is plotted as a function of X ($[V_{total}]$ is the total concentration of vanadium, i.e., equal to $[V^{4+}] + [V^{5+}]$). Initially as X increases, $[V^{4+}]/[V_{total}]$ remains constant at around 5%. At $X = 0.45$ an abrupt change in slope occurs, and the $[V^{4+}]/[V_{total}]$ ratio drastically decreases with further increase in X. $[V^{4+}]/[V_{total}]$ is defined as c of the Mott–Austin equation (eq 3).

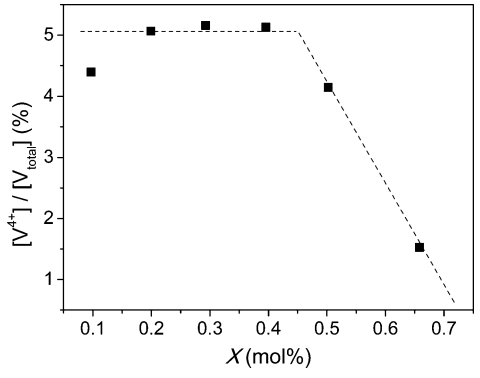

Figure 4. Redox ratio of $[V^{4+}]/[V_{total}]$, where $[V_{total}]$ is the total amount of vanadium ions, as a function of X (=$[V_2O_5]/([V_2O_5] + [TeO_2])$). $[V^{4+}]/[V_{total}]$ is expressed as parameter c in the Mott–Austin equation (eq 3). The dashed line is a guide for the eyes.

Liquid fragility index (m) of the glass systems is determined by a linear fit of the viscosity data around T_g (see inset of Figure 5), i.e., through the following relation:[36]

$$m \equiv \left.\frac{\partial(\log \eta(T))}{\partial(T_g/T)}\right|_{T=T_g} \quad (2)$$

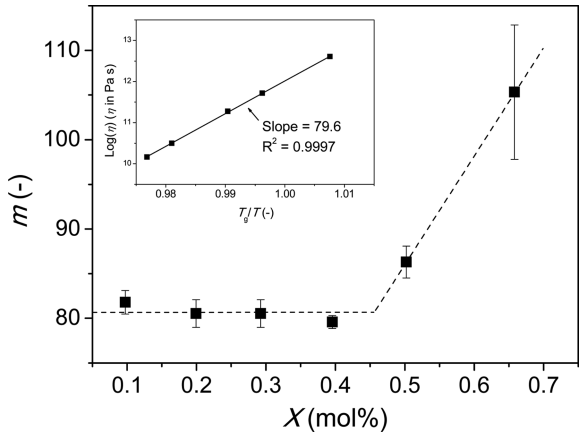

Figure 5. Liquid fragility index (m) as a function of the molar concentration X (=$[V_2O_5]/([V_2O_5] + [TeO_2])$). Inset: Determination of m using eq 2 by taking the 40 mol % V_2O_5 containing glass as an example. The dashed line is a guide for the eyes showing the compositional scaling of m.

The dependence of m on V_2O_5 content is illustrated in Figure 5. m remains unchanged at ∼80 for X between 0.1 and 0.45 but drastically increases linearly up to m = 105 when X increases from 0.45 to 0.65. Supposing that this trend continues, vitreous V_2O_5 would have an m value of 147.

Since H_v strongly depends on the condition of indentation,[37,38] all microindentation experiments were performed with the same indentation load and time (0.25 N and 10 s), ensuring crack free indents. The H_v values are plotted in Figure 6 as a function of X. H_v remains constant when X increases from 0.1 to 0.45, followed by a linear decrease with further increasing X from 0.45 to 0.65. Considering the experimental error associated with the hardness determinations, the compositional hardness scaling agrees with that reported in

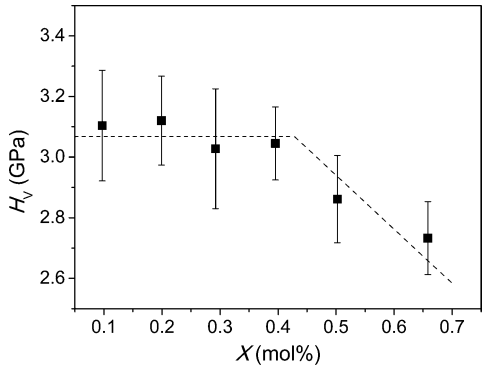

Figure 6. Vickers hardness (H_v) as a function of X (=$[V_2O_5]/([V_2O_5] + [TeO_2])$) of the six vanadium tellurite glasses. The dashed line is a guide for the eye.

dx.doi.org/10.1021/jp508910m | J. Phys. Chem. B 2014, 118, 14942–14948

literature,[22,23] viz., a decrease in H_v with increasing X. The compositional behavior of H_v (Figure 6) resembles that of c (Figure 4), i.e., an initial plateau followed by a decrease with further increase in X.

Room temperature density and molar volume (V_m) are presented in Figure 7. V_m is calculated as the molar mass divided by the glass density. Density exhibits a linear decrease with increasing X, whereas the molar volume increases nonlinearly.

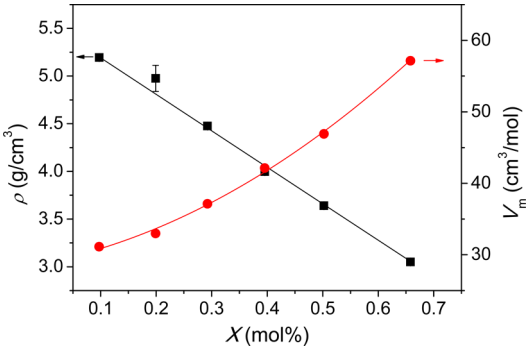

Figure 7. Room temperature density (ρ) and molar volume (V_m) as a function of X (=$[V_2O_5]/([V_2O_5] + [TeO_2])$) for the six vanadium tellurite glasses. Solid lines represent the trends in the respective properties.

Electronic conductivity of glasses containing transition metal oxide is evaluated via the Mott–Austin equation (eq 3).[42,43]

$$\sigma = \left(\frac{\nu_0 e^2}{Rk_bT}\right) c(1-c)\, e^{-2\alpha R}\, e^{-W/(k_bT)} \quad (3)$$

where ν_o is the optical phonon frequency, R is the mean distance between the ions where the electron transfer occurs (vanadium ions in this case), α is the tunneling factor, and W is the activation energy. The parameters of the Mott–Austin equation can be determined by plotting $\log(\sigma T)$ vs $1000/T$ and fitting eq 3 to each set of conductivity data. This is performed in Figure 8, and the derived parameters are shown in Table 3. In order only to have two fitting parameters (namely, α and ν_0),

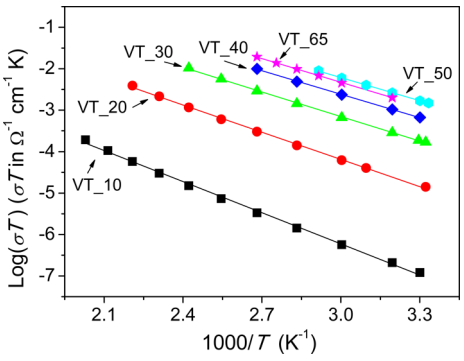

Figure 8. Logarithm of electronic conductivity times temperature ($\log(\sigma T)$) as a function of inverse temperature ($1000/T$) for the vanadium tellurite glasses. The sample identities are indicated in the figure, and the compositions are tabulated in Table 1. The Mott–Austin equation (eq 3) is fitted to each composition via the least-squares method and plotted as solid lines. Regression data are shown in Table 3.

c and R are determined by EPR and pycnometry, respectively. R is calculated as per eq 4:[44,45]

$$R = \left(\frac{M_W}{2M_e\rho N_v}\right)^{1/3} \quad (4)$$

where M_W is the molar mass, M_e the molar concentration of conductive sites (i.e., vanadium), ρ the density, and N_v Avogadro's constant. R is plotted in the inset of Figure 9 and c values are plotted in Figure 4. In Figure 8 it is seen that the electronic conductivity of the vanadium tellurite glasses increases with X. The observed increase in electronic conductivity with increasing V_2O_5 is in good agreement with that reported elsewhere.[3,5,7−9] In order to better visualize this correlation, electronic conductivity data at 298 K (σ_{298K}), along with W, are plotted in Figure 9 as a function of X. The $\log(\sigma_{298K})$ initially increases with X, while W decreases. Both quantities reach a plateau when X surpasses the critical value of about 0.45.

4. DISCUSSION

The decrease in ρ with increasing X (Figure 7) indicates a looser packing of the atoms, since the molar mass of V_2O_5 is higher than that of TeO_2. The observed increase in V_m implies that V_2O_5 constitutes a less compact structural arrangement. The structural expansion with increasing X causes a decrease in the bond numbers per unit volume, i.e., a decrease of constraints, and hence a decrease in T_g (Figure 2 and Table 2).[46−48] The decrease of ρ and T_g with increasing X has also been reported in previous studies,[3,28,39−41] e.g., T_g drops from 560 to 505 K when V_2O_5 is raised from 10 to 50 mol %.[26] In contrast, the onset temperature of crystallization (T_c) first decreases with X and then increases (Table 2). The melting temperature (T_m) only slightly varies in an irregular manner. Consequently, according to eq 1, the glass stability parameter (K_H) first increases and then decreases with increasing X. The trend manifests itself as a Gaussian distribution of K_H over X with a maximum around X = 0.3 (Table 2). This is consistent with a previous study,[27] but different from another study,[28] where the glass stability is found to linearly increase with increasing X.

Vanadium tellurite glasses have been reported to contain both VO_4 and VO_5 polyhedra,[22−26,46] where V^{4+} primarily exists in tetragonally distorted octahedral coordination,[22,25] and V^{5+} mainly exists in a trigonal bipyramidal configurational (~80%) at low V_2O_5 concentrations. As the V_2O_5 concentration increases, the energetically preferred coordination geometry of V^{5+} however changes from a trigonal bipyramidal coordination at low V_2O_5 concentrations to a 50/50 mixture of trigonal bipyramidal and tetrahedral configuration at high V_2O_5 concentrations.[24,28] By comparison of ρ and c obtained in this work with the structural environment of vanadium in vanadium tellurite glass obtained in literature,[22−26,28] an increase in tetrahedral sites could cause an expansion of the glass network (Figure 7) and consequently decrease the amount of bonds per unit volume (decrease in connectivity and T_g; see Figure 2).[23,28] If all V^{4+} ions are assumed to occupy tetragonally distorted octahedral sites, from Figure 4 we can infer that the fraction of distorted tetrahedral sites starts to drop at X = 0.45.

At a certain c value, the V^{4+} ions start to contribute more constraints to the network than V^{5+}, leading to the onset of both the increase in m (Figure 5) and the drop in H_v (Figure 6) at about X = 0.45. When the fraction of tetragonal V^{4+} sites

dx.doi.org/10.1021/jp508910m | J. Phys. Chem. B 2014, 118, 14942−14948

Table 3. Electronic Conductivity at 298 K (σ_{298K}), Pre-Exponential Term (σ_0), and Activation Energy (W) of the Mott Equation, Tunneling Factor (α), Phonon Frequency (ν_0), and Adjusted Sum of Squared Errors (SSQE) Determined via Fitting of Eq 3 to Electronic Conductivity Data[a]

sample identification	$\log(\sigma_0)$ [σ_0 in Ω^{-1} cm^{-1}]	W [eV]	$\log(\sigma_{298K})$ [σ_{298K} in Ω^{-1} cm^{-1}]	c [%]	R [nm]	α [cm^{-1}]	ν_0 [s^{-1}]	SSQE [−]
VT_10	1.29	0.50	−7.12	4.40	0.64	1.7×10^{-9}	1.6×10^{10}	0.9980
VT_20	2.37	0.43	−4.97	5.07	0.52	1.0×10^{-8}	1.4×10^{11}	0.9987
VT_30	2.78	0.39	−3.86	5.16	0.47	7.4×10^{-9}	3.2×10^{11}	0.9992
VT_40	3.04	0.37	−3.29	5.13	0.45	2.7×10^{-8}	5.5×10^{11}	0.9996
VT_50	3.36	0.37	−2.88	4.15	0.43	1.0×10^{-8}	1.3×10^{12}	0.9995
VT_65	3.39	0.38	−3.00	1.53	0.42	1.7×10^{-7}	3.7×10^{12}	0.9997

[a] R is the mean distance between vanadium ions (from density data and eq 4), and c is the ratio of V^{4+} to total vanadium (from EPR measurements).

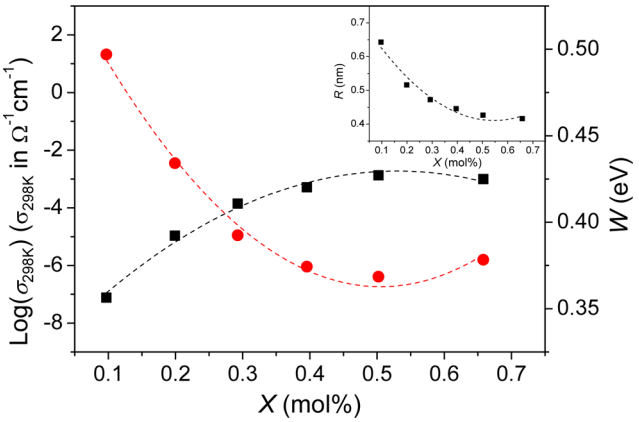

Figure 9. Logarithm of electronic conductivity at 298 K ($\log(\sigma_{298K})$) and activation energy of electronic conduction (W) as a function of X (=[V_2O_5]/([V_2O_5] + [TeO_2])). The $\log(\sigma_{298K})$ is plotted in the primary ordinate and W on the secondary. Inset: Mean distance between vanadium ions (R) as a function of X. The dashed lines are guides for the eyes.

starts to decrease, the quantity of the most constrained network diminishes, leading to a decrease in H_v and an increase in m. Sharma et al.[23] measured H_v and c of vanadium phosphate, vanadium tellurite, and vanadium borate glasses and found that in these systems the c value decreases with an increase in X, almost parallel to a 1:1 decrease in H_v. As demonstrated in Figures 5 and 6, the ratio of V^{4+} to total vanadium is seen to have significant impact on both H_v and m. According to Figures 4−6 and a previous work,[23] c is believed to impact the physical and dynamic properties of the studied glass, since it affects the structure of these glasses. For the three different vanadium systems, an approximate 1:1 correlation is found between H_v, m, and c.

A change of c affects the local structural arrangements in the studied glasses and hence results in a mismatch in constraints between the two involved structural arrangements (i.e., V^{4+} in tetragonally distorted octahedral coordination and V^{5+} in a trigonal bipyramidal coordination). As both H_v and m have been shown to linearly depend on the total amount of constraints in the network,[47,48] a direct link might occur between H_v, m, and c. H_v and m are measured at different temperatures, but the structural arrangements that c differentiates between might exhibit a constraint mismatch both at room temperature and at T_g. The m value of the vanadium tellurite glass with 40 mol % V_2O_5 was found by Souri to be 70.[4] This m value is only slightly lower than that shown in Figure 5 considering the relatively large error range of m.

Consistent with the change of the kinetic fragility (m), the C_p jump across the glass transition (ΔC_p) (see Table 2) also increases with increasing X. ΔC_p is a measure of the thermodynamic fragility. This implies that the change of the configurational entropy during the glass transition is associated with that of the valence state of the vanadium. This means that the change of the local structural environment scales with the change in the configurational entropy.

In contrast, electronic conductivity does not show the same compositional trend as H_v and m, indicating that other structural factors rather than c dictates the electronic conductivity. As shown in Figure 9, the electronic conductivity measured at 298 K ($\log(\sigma_{298K})$) initially increases with X and then remains almost unchanged above $X = 0.45$, exactly where c drastically drops. This is surprising, as eq 3 predicts an increase in $\log(\sigma_{298K})$ with increasing c (for $c < 0.5$). The compositional scaling of $\log(\sigma_{298K})$ matches that of the mean distance between vanadium ions (R) (see inset of Figure 9), since eq 3 predicts R and $\log(\sigma_{298K})$ to be inversely proportional. The exact same trend is observed for W (Figure 9), and the linear relation between W and R is well documented for vanadium tellurite glasses.[7,9,49,50] On the basis of Figures 8 and 9, we can infer that the electronic conductivity of the vanadium tellurite glasses depends linearly on R. This is not surprising, as the electron hopping is strictly adiabatic, as $\exp(-2\alpha R) = 1$ for all compositions (see Table 3). In the adiabatic case we expect a linear influence of R on σ. The fact that electron hopping occurs adiabatically in vanadium tellurite glass is in good agreement with former measurements.[44,51,52] In order to achieve higher conductivity, the vanadium ions must thus be brought closer to each other, i.e., an increase in density. This implies that the electronic conductivity is not so dependent on c as predicted by the Mott−Austin equation (eq 3). When c varies, VO_4 and VO_5 polyhedra are interchanging, leading to changes in R. It might be this change in R that facilitates the changes in $\log(\sigma_{298K})$.[9,11,19−21,49,50] For an electrochemical application, e.g., cathode materials in secondary lithium batteries, it is important to optimize the relevant properties such as m, H_v, and σ of the vanadium tellurite glass. This work contributes to establishing the knowledge basis for designing battery materials. Certainly, further studies still need to be done in order to clarify the detailed microscopic mechanism of the abrupt change of the studied properties at the critical V_2O_5 concentration. In particular, a detailed structure analysis by small angle neutron/X-ray diffraction techniques and molecular dynamic modeling will provide additional information on the role of the structure in determining the properties of the vanadium tellurite glass systems.[53,54]

dx.doi.org/10.1021/jp508910m | J. Phys. Chem. B 2014, 118, 14942−14948

5. CONCLUSION

We have observed a critical V_2O_5 concentration in the vanadium tellurite glasses, above which the local structure undergoes a drastic change, leading to an abrupt change in both physical and dynamic properties.

Hardness and liquid fragility of the studied glasses remain almost unchanged with X when $X < 0.45$. However, when X exceeds 0.45, hardness drops whereas the liquid fragility rises. This means that there is a critical V_2O_5 concentration of $X = 0.45$, above which an abrupt change of the glass properties takes place. The observed trends in hardness and liquid fragility are closely related to the valence ratio of the vanadium ions (c), as c shows the same trend. The reason for this coincidence could be that V^{4+} results in a more constrained structure than V^{5+}, i.e., in fewer constraints per unit volume and hence in lower hardness and higher fragility.

The electronic conduction of vanadium tellurite glasses occurs strictly adiabatically, and σ does not follow the expected correlation to c as predicted by the Mott–Austin equation; instead it exhibits a linear correlation to R. If the decoupling of σ from c also occurs at higher c values, it enables optimization of hardness and liquid fragility without influencing σ.

AUTHOR INFORMATION

Corresponding Author

*Phone: +45 9940 8522. E-mail: yy@bio.aau.dk.

Notes

The authors declare no competing financial interest.

ACKNOWLEDGMENTS

S.M. gratefully acknowledges Carlsbergfondet and the Danish Independent Research Council (Grants DFF-09-070250 and DFF-1335-00175) for supporting the EPR facility at DTU Chemistry. A.C.M.R. acknowledges Fapesp-Cepid, Process No. 2013/07793-6.

REFERENCES

(1) Levy, M.; Souquet, J. L. Amorphous and Vitreous Materials as Electrodes in Electrochemical Cells. *Mater. Chem. Phys.* **1989**, *23*, 171–188.

(2) Lebrun, N.; Levy, M.; Souquet, J. L. Electrical Conductivity in Glasses of the TeO_2-V_2O_5-MoO_3 System. *Solid State Ionics* **1990**, *40/41*, 718–722.

(3) Kumar, M. P.; Sankarappa, T.; Awasthi, A. M. Thermal and Electrical Properties of Some Single and Mixed Transition-Metal Ions-Doped Tellurite Glasses. *Physica* **2008**, *B403*, 4088–4095.

(4) Souri, D. Glass Transition and Fragility of Telluro-Vanadate Glasses Containing Antimony Oxide. *J. Mater. Sci.* **2012**, *47*, 625–631.

(5) Sankarappa, T.; Kumar, M. P.; Devidas, G. B.; Nagaraja, N.; Ramakrishnareddy, R. AC Conductivity and Dielectric Studies in V_2O_5–TeO_2 and V_2O_5–CoO–TeO_2 Glasses. *J. Mol. Struct.* **2008**, *889*, 308–315.

(6) Chopra, N.; Mansingh, A.; Chadha, G. K. Electrical, Optical and Structural Properties of Amorphous V_2O_5-TeO_2 Blown Films. *J. Non-Cryst. Solids* **1990**, *126*, 194–201.

(7) Souri, D. Small Polaron Hopping Conduction in Tellurium Based Glasses Containing Vanadium and Antimony. *J. Non-Cryst. Solids* **2010**, *356*, 2184–2184.

(8) Levy, M.; Rousseau, F.; Duclot, M. J. Electrochemical Properties of Glasses in the TeO_2-V_2O_5 System. *Solid State Ionics* **1988**, *28–30*, 736–738.

(9) Dhawan, V. K.; Mansingh, A.; Sayer, M. DC Conductivity of V_2O_5-TeO_2 Glasses. *J. Non-Cryst. Solids* **1982**, *51*, 87–103.

(10) Chung, C. H.; Mackenzie, J. D. Electrical Properteis of Binary Semiconducting Oxide Glasses Containing 55 Mole % V_2O_5. *J. Non-Cryst. Solids* **1980**, *42*, 357–370.

(11) El-Desoky, M. M. Potassium Doping of Semiconducting Vanadium Tellurate Glasses. *Mater. Chem. Phys.* **2002**, *73*, 259–262.

(12) Jayasinghe, G. D. L. K.; Dissanayake, M. A. K. L.; Careem, M. A.; Souquet, J. L. Electronic to Ionic Conductivity of Glasses in the Na_2O-V_2O_5-TeO_2 System. *Solid State Ionics* **1997**, *93*, 291–295.

(13) Montani, R. A.; Lorente, A.; Vincenzo, M. A. Effect of Ag_2O on the Conductive Behaviour of Silver Vanadium Tellurite Glasses. *Solid State Ionics* **2000**, *130*, 91–95.

(14) Montani, R. A.; Levy, M.; Souquet, J. L. An Electrothermal Model for High-Field Conduction and Switching Phenomena in TeO_2-V_2O_5 Glasses. *J. Non-Cryst. Solids* **1992**, *149*, 249–256.

(15) Kumar, M. P.; Sankarappa, T. DC Conductivity in Some Alkali Doped Vanadotellurite Glasses. *Solid State Ionics* **2008**, *178*, 1719–1424.

(16) Ghosh, A.; Chakravorty, D. Semiconducting Properties of Sol-Gel Derived Vanadium Silicate Glasses. *Appl. Phys. Lett.* **1991**, *59*, 855–856.

(17) Sayer, M.; Mansingh, A. Transport Properties of Semiconducting Phosphate Glasses. *Phys. Rev.* **1972**, *B6*, 4629–4643.

(18) Sharma, B. K.; Dube, D. C.; Mansingh, A. Preparation and Characterization of V_2O_5-B_2O_3 Glasses. *J. Non-Cryst. Solids* **1984**, *65*, 39–51.

(19) Bandyopadhyay, A. K.; Isard, J. O.; Perke, S. Polaronic Conduction and Spectroscopy of Borate Glasses Containing Vanadium. *J. Phys. D: Appl. Phys.* **1978**, *11*, 2559–2576.

(20) Linsley, G. S.; Owen, A. E.; Hayatee, F. M. Electronic Conduction in Vanadium Phosphate Glasses. *J. Non-Cryst. Solids* **1970**, *4*, 208–219.

(21) Munakata, M. Electrical Conductivity of High Vanadium Phosphate Glass. *Solid-State Electron.* **1960**, *1*, 159–163.

(22) Chopra, N.; Mansingh, A.; Mathur, P. Electron Paramagnetic Resonance and Microhardness of Binary Vanadium Tellurite Glasses. *J. Non-Cryst. Solids* **1992**, *146*, 261–266.

(23) Sharma, B. I.; Robi, P. S.; Srinivasan, A. Microhardness of Ternary Vanadium Pentoxide Glasses. *Mater. Lett.* **2003**, *57*, 3504–3507.

(24) Hoppe, U.; Yousef, E.; Rüssel, C.; Neuefeind, J.; Hannon, A. C. Structure of Vanadium Tellurite Glasses Studied by Neutron and X-ray Diffraction. *Solid State Commun.* **2002**, *123*, 273–278.

(25) Baia, L.; Bolboaca, M.; Kiefer, W.; Yousef, E. S.; Rüssel, C.; Breitbarth, F. W.; Mayerhöfer, T. G.; Popp, J. Spectroscopic Studies on the Structure of Vanadium Tellurite Glasses. *Phys. Chem. Glasses* **2004**, *45*, 178–182.

(26) Sakida, S.; Hayakawa, S.; Yoko, T. ^{125}Te and ^{51}V Static NMR Study of V_2O_5–TeO_2 Glasses. *J. Phys.: Condens. Matter* **2000**, *12*, 2579–2595.

(27) El-Moneim, A. A. DTA and IR Absorption Spectra of Vanadium Tellurite Glasses. *Mater. Chem. Phys.* **2002**, *73*, 318–322.

(28) El-Mallawany, R. Glass Transformation Temperature and Stability of Tellurite Glasses. *J. Mater. Res.* **2003**, *18*, 402–406.

(29) Kjeldsen, J.; Yue, Y. Z.; Bragatto, C. B.; Rodrigues, A. C. M. Electronic Conductivity of Vanadium-Tellurite Glass-Ceramics. *J. Non-Cryst. Solids* **2013**, *378*, 196–200.

(30) Yue, Y. Z.; Christiansen, J. D.; Jensen, S. L. Determination of the Fictive Temperature for a Hyperquenched Glass. *Chem. Phys. Lett.* **2002**, *357*, 20–24.

(31) Zheng, Q.; Potuzak, M.; Mauro, J. C.; Smedskjaer, M. M.; Youngman, R. E.; Yue, Y. Z. Composition–Structure–Property Relationships in Boroaluminosilicate Glasses. *J. Non-Cryst. Solids* **2012**, *358*, 993–1002.

(32) Hrüby, A. Evaluation of Glass-Forming Tendency by Means of DTA. *J. Phys. (Paris)* **1972**, *B22*, 1187–1193.

(33) Marques, T. V. R.; Cabral, A. A. Influence of the Heating Rates on the Correlation Between Glass-Forming Ability (GFA) and Glass Stability (GS) Parameters. *J. Non-Cryst. Solids* **2014**, *390*, 70–76.

(34) Nascimento, M. L. F.; Souza, L. A.; Ferreira, E. B.; Zanotto, E. D. Can Glass Stability Parameters Infer Glass Forming Ability? *J. Non-Cryst. Solids* **2005**, *351*, 3296−3308.
(35) Chase, G. A.; Phillips, C. J. Equilibrium in the Glass-Forming System TeO_2-V_2O_5. *J. Am. Ceram. Soc.* **1964**, *47*, 467.
(36) Angell, C. A. Formation of Glasses from Liquids and Biopolymers. *Science* **1995**, *267*, 1924−1935.
(37) Kavetskyy, T.; Borc, J.; Sangwal, K.; Tsmots, V. Indentation Size Effect and Vickers Microhardness Measurement of Metal-Modified Arsenic Chalcogenide Glasses. *J. Optoelectron. Adv. Mater.* **2010**, *12*, 2082−2091.
(38) Schneider, J.-M.; Bigerelle, M. Statistical Analysis of the Vickers Hardness. *Mater. Sci. Eng., A* **1999**, *262*, 256−263.
(39) El-Mallawany, R. Specific Heat Capacity of Semiconducting Glasses: Binary Vanadium Tellurite. *Phys. Status Solidi* **2000**, *177*, 439−444.
(40) Rada, S.; Rada, M.; Cuela, E. Infrared Spectroscopic and DFT Investigations of the Vanadate-Tellurate Glasses Structures. *Spectrochim. Acta* **2010**, *A75*, 846−851.
(41) Sidkey, M. A.; El-Mallawany, R.; Nakhla, R. I.; El-Moneim, A. A. Ultrasonic Studies of $(TeO_2)_{1-x}$-$(V_2O_5)_x$ glasses. *J. Non-Cryst. Solids* **1997**, *215*, 75−82.
(42) Mott, N. F. Electrons in Disordered Structures. *Adv. Phys.* **1967**, *16*, 49−144.
(43) Austin, I. G.; Mott, N. F. Polarons in Crystalline and Non-Crystalline Materials. *Adv. Phys.* **1969**, *18*, 41−102.
(44) Mori, H.; Matsuno, H.; Sakata, H. Small Polaron Hopping Conduction in V_2O_5-Sb-TeO_2 Glasses. *J. Non-Cryst. Solids* **2000**, *276*, 78−94.
(45) Hirashima, H.; Arai, D.; Yoshida, T. Electrical Conductivity of PbO-P_2O_5-V_2O_5 Glasses. *J. Am. Ceram. Soc.* **1985**, *68*, 486−489.
(46) Mauro, J. C. Topological Constraint Theory of Glass. *Am. Ceram. Soc. Bull.* **2011**, *90*, 31−37.
(47) Smedskjaer, M. M.; Mauro, J. C.; Sen, S.; Yue, Y. Z. Quantitative Design of Glassy Materials Using Temperature-Dependent Constraint Theory. *Chem. Mater.* **2010**, *22*, 5358−5365.
(48) Smedskjaer, M. M.; Mauro, J. C.; Yue, Y. Z. Prediction of Glass Hardness Using Temperature-Dependent Constraint Theory. *Phys. Rev. Lett.* **2010**, *105*, 115503.
(49) Mori, H.; Kitami, T.; Sakata, H. Electrical Conductivity of V_2O_5-Bi_2O_3-TeO_2 Glasses. *J. Ceram. Soc. Jpn.* **1992**, *101*, 338−343.
(50) Sakata, H.; Amano, M.; Yagi, T. DC Conductivity of V_2O_5-PbO-TeO_2 Glasses and the Effect of Pressure. *J. Non-Cryst. Solids* **1996**, *194*, 198−206.
(51) Mori, H.; Kitami, T.; Sakata, H. Electrical Conductivity of V_2O_5-Sb_2O_3-TeO_2 Glasses. *J. Non-Cryst. Solids* **1994**, *168*, 157−166.
(52) Moawad, H. M. M.; Jain, H.; Mallawany, R. E.; Ramadan, T.; Sharbiny, M. E. Electrical Conductivity of Silver Vanadium Tellurite Glasses. *J. Am. Ceram. Soc.* **2002**, *85*, 2655−2659.
(53) Matsumoto, H.; Mabuchi, T.; Shigesato, Y.; Yasui, I. Structure Analysis of ZnO-TeO_2 Glasses by Means of Neutron Diffraction and Molecular Dynamics. *Jpn. J. Appl. Phys.* **1996**, *35*, 694−698.
(54) Ori, G.; Montorsi, M.; Redone, A.; Siligardi, C. Insight into the Structure of Vanadium Containing Glasses: A Molecular Dynamics Study. *J. Non-Cryst. Solids* **2011**, *357*, 2571−2579.